

Particle motions on a plane floor under waves

Kao-Shu, Hwang Hwung-Hweng, Hwung & Po-Ching, Huang
Tainan Hydraulics Laboratory, National Cheng Kung University, Tainan, Taiwan.

ABSTRACT: The motion of spherical particles on a plane floor subjected to waves was investigated. The testing program included a single sphere, two spheres and multiple spheres with different initial space arrangement. An image processing system was used to record and analyze the particle wavelengths in multiple spheres cases and to reveal the paths of the particle motions in cases with a single sphere. For multiple spheres, they broke into groups first then each group aligned in traverse direction and formed a periodic pattern in space which was called particle waves. The stable particle wavelength can be expressed as a function of the water particle excursion distance at bottom. Two spheres initially aligned in the wave propagation direction would finally turn to be side by side in a line that is perpendicular to the wave propagation direction. The path of a single sphere shows that the particle would move in both longitudinal and traverse directions. Its mean forward component in longitudinal direction and the mean amplitude of displacement are proportional with Shields parameter. The lateral component of displacement, on the other hand, seemed not to follow a certain rule.

1. INTRODUCTION

The study of particle motion in flows is practical in a variety of applications, such as particle-laden flows in the field of chemical engineering and coastal or hydraulics engineering. For example, sand ripples are common features happened on most fluid-sand interface. In a study on the initiation of ripple marks, Kaneko and Honji (1979a) has showed that a single-layer of initially scattered glass beads would eventually grow into regular waves of particles under oscillating flows. Hwang (1995) also indicated that such a phenomenon happened prior to the well-recognized “rolling grain ripple”, which was first defined by Bagnold (1946). And this negligible development is indeed the key process dominating the entire sandy ripple formation. Figure 1 is an example qualitatively showing the evolution process of spheres subjected to waves. A group of spheres were initially aligned in the direction of waves (Figure 1a). The spheres then broke into sub-groups within a couple waves (Figure 1b, Figure 1c). Then each sub-group aligned in traverse direction (Figure 1e) and formed the very primary pattern of ripple marks (Figure 1f). Wunenburger et al. (2002) conducted experiments with metal spheres in a rectangular box which filled with water. The spheres were observed to form periodic order chains which oriented perpendicular to the oscillating direction as the box oscillated periodically. They concluded that the formation of steady streaming, as shown in Sleath (1976) and Kaneko and Honji (1979b) on investigating the oscillatory viscous flow over a wavy wall, may be linked to the onset of this periodic pattern.

Apart from the complex mechanisms that may involved, ex., the interaction between the spheres and the oscillatory boundary layer flows, the transport modes of the spheres ...etc., the phenomenon that the spheres not only transported longitudinally but also laterally is the most striking point that is worthy of much more in depth study. Sarpkaya (1975) measured the forces

on spheres in an oscillatory flow. The force coefficients of the in-line forces was reported to follow the same trend as those for cylinders, but there was no discussion on the side forces due to its complexity. The motion of a sphere on a plane boundary in oscillatory flow was investigated by Martin et. al. (1976). They found that the rotational effect of the fluid would cause the inertia coefficient to be higher for rotating spheres than for stationary or translating spheres. The behavior of spheres sedimenting between two infinite vertical walls in a viscous fluid was reported by Vasseur and Cox (1977). Their theoretical implementation suggested that attractive forces in the flow direction and weakly repulsive forces in the traverse direction would result in the two spheres approaching each other perpendicularly to the flow direction. On the other hand, interesting experiments performed by Joseph et al. (1994) showed that when there were two spheres fall side by side in a viscoelastic liquid, the two bodies can result in an attractive force which causes them to migrate towards each other. That is, the two spheres became one on top with its bottom contact with the top of the other one in a line parallel to the falling direction. Using the same experimental set-up but with a viscous Newtonian fluid, however, they found the two spheres repelled each other.

Several other theoretical or numerical approaches and few experiments were reported with the motion of single or multiple spheres in the gravitational environment, as reviewed by Sun and Chwang (2006). Much more simplified but profound studies were those which focused on the flow field about viscous flows passing a fixed sphere. Johnson and Patel (1999) investigated the flow of an incompressible viscous fluid past a sphere. Experimental and computational results showed that at lower Reynolds numbers, the wake behind the sphere is steady and symmetric; when Reynolds number is larger than 210, the wake becomes asymmetric. As $Re > 280$, the wake pattern becomes unsteady, with hairpin structures forming in the wake. Unsteady axis-symmetric viscous flow past a rigid sphere was investigated by Chang and Maxey (1994). They showed that separation forms at lower Reynolds numbers in an oscillatory flow than in steady flows.

The objective of this study is to look into the behavior of spheres which initially rested on a plane floor then subjected to waves. Based on the above-mentioned qualitative results by Hwang (1995) and to go beyond, tests with different Shields parameters and relative roughness were conducted in a wave flume. Macroscopic particle wave formation features are discussed for cases with multiple spheres. While for the cases with a single sphere, more details about the paths are displayed.

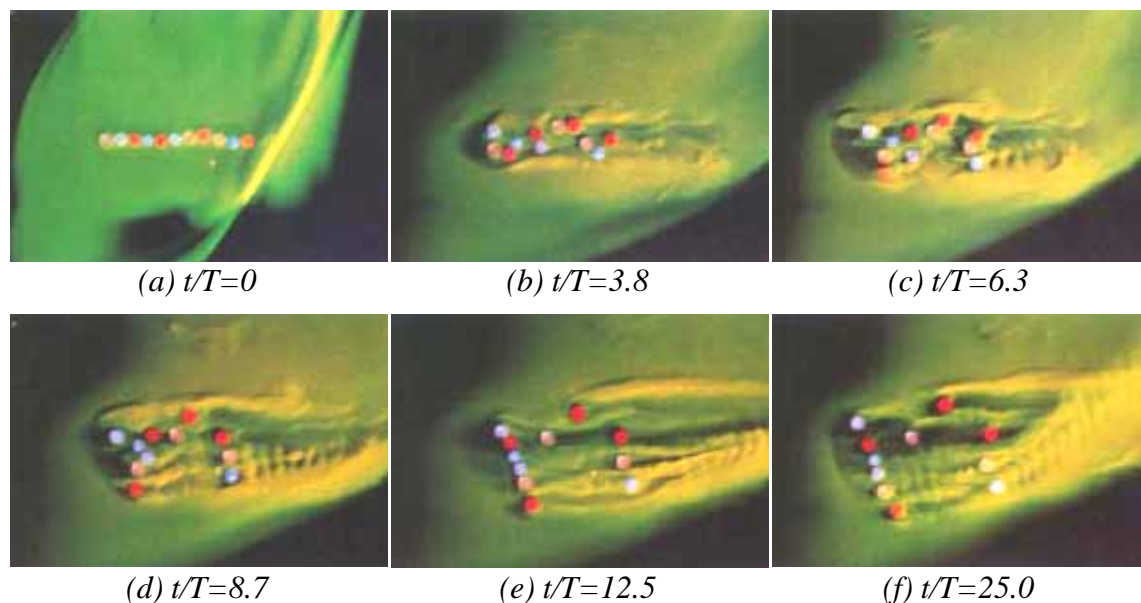


Figure 1 Visualization of the motion of initially longitudinally aligned spheres subjected to waves (T : wave period, t : time elapsed in second).

2. DIMENSIONAL ANALYSIS

For spheres initially rest on a plane bottom then subjected to waves, the associated variables include: the fluid density, ρ , the kinematic viscosity of the fluid, ν , the wave periods, T , the wave height, H , the water depth, h , the gravity, g , the density of the sphere, ρ_s , and the diameter of the sphere, D . Considering the motions in a wave boundary layer, the excursion length of water particles on the bottom, a , and the correspondent velocity amplitude, U_b , were used. Where

$$a = \frac{H}{2 \sinh \frac{2\pi}{L} h} \quad (1)$$

$$U_b = \frac{2\pi a}{T} \quad (2)$$

Moreover, the submerged specific weight of the spheres, γ_s , was used.

$$\gamma_s = (\rho_s - \rho)g \quad (3)$$

Variables about the evolution of spheres under waves can be expressed as :

$$f = (\rho, \nu, a, U_b, h, \gamma_s, D) \quad (4)$$

Dimensionless parameters were then obtained by π theory.

$$\frac{DU_b}{\nu}, \frac{\rho U_b^2}{\gamma_s D}, \frac{a}{D}, \frac{\rho_s}{\rho}, \frac{h}{D} \quad (5)$$

A similar parameter to the second parameter above is Shields parameter:

$$\psi = \frac{\tau_0}{\gamma_s D} = \frac{u_*^2}{(s-1)gD} = \frac{f_w U_b^2}{2(s-1)gD} = \frac{f_w}{2} \Phi \quad (6)$$

where f_w is the friction coefficient and Φ is the mobility number, the second term in eq. (5).

3. EXPERIMENTAL SET-UP

The experiments were carried out in a wave flume of 9.5 m long, 0.3 m wide and 0.7 m high. Regular waves were generated by a piston type wave maker. To minimize the reflection waves, an energy dissipating beach with armour units, porous stainless plates and sponge were installed at the other end of this flume. For all the experiments, measured wave reflection coefficients were under 5%. The both sides and part of the bottom of the flume was made of reinforced glass that made the observation either from the side walls or under the flume possible. The motions of spheres were recorded by an image processing system. This system included a 500-watts light source, a CCD camera (Sony XC-77RR) and a frame grabber. The frame rate was 30 frames/s with a shuttle speed of 1/250 s. Sequential images were stored in the memory then output frame by frame. The paths of spheres were then calculated by a particle tracing algorithm. The schematic diagram of the experimental set-up is illustrated in Figure 2.

The test conditions are listed in Table 1. Three kinds of spheres of which diameter were 1.0 mm but with different densities were used. Among the three, the lightest one was the acrylic sphere, of which density is 1.03. Then a kind of plastic resin sphere, of which density is 1.42, was used. The third one was the glass bead, of which density is 2.46. Waves of different wave heights and wave periods were generated. The Shields parameters ranged from 0.01 to 1.53.

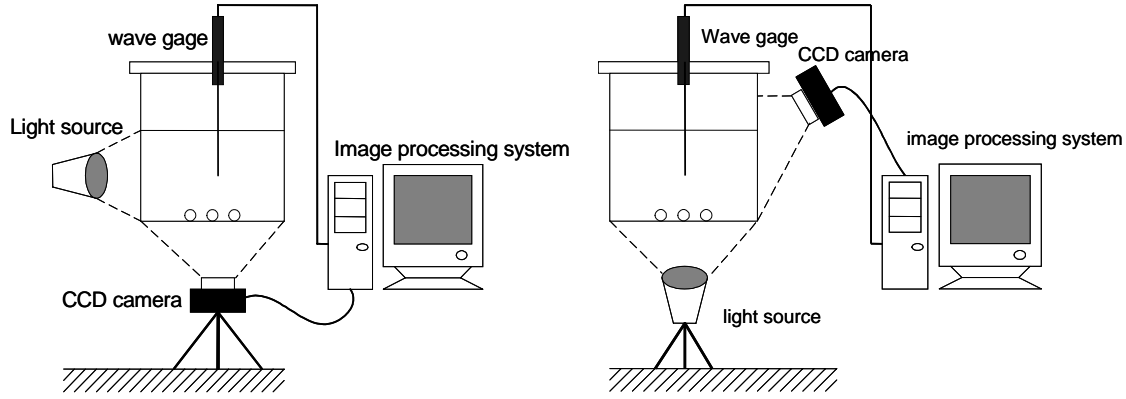


Figure 2 Schematic diagram of experimental set-up.

Table 1 Test conditions

case	sphere type	h (cm)	T (sec)	H (cm)	a (cm)	U_b (cm/s)	ρ_s	D (mm)	ψ	Re
T1	acrylic sphere	15	0.97	1.02	0.50	3.2	1.03	1.0	0.37	30.5
T2	acrylic sphere	15	0.97	1.87	0.91	5.6	1.03	1.0	0.70	53.1
T3	acrylic sphere	20	1.07	4.65	2.11	12.4	1.03	1.0	1.53	116.8
T4	plastic resin sphere	15	0.97	2.04	1.0	5.3	1.42	1.0	0.05	50.1
T5	plastic resin sphere	20	0.94	3.96	1.44	9.0	1.42	1.0	0.08	85.1
T6	plastic resin sphere	20	1.11	4.41	2.13	12.1	1.42	1.0	0.11	113.7
T7	plastic resin sphere	20	1.20	5.13	2.78	14.5	1.42	1.0	0.11	137.3
T8	plastic resin sphere	30	1.11	8.77	2.97	16.8	1.42	1.0	0.16	158.5
T9	glass bead	15	0.97	1.94	0.95	5.6	2.46	1.0	0.01	53.1
T10	glass bead	20	0.86	4.02	1.22	8.9	2.46	1.0	0.02	84.0
T11	glass bead	20	1.11	4.41	2.13	12.1	2.46	0.1	0.03	11.4
T12	glass bead	20	1.20	5.04	2.73	14.3	2.46	0.1	0.03	13.5
T13	glass bead	20	1.46	5.86	4.16	17.9	2.46	0.1	0.04	16.9

4. RESULTS AND DISCUSSION

Figure 3 (a)~(d) show the evolution processes of initially scattering plastic resin spheres subjected to waves (case T5). Initially, a single layer of spheres were randomly scattered on the floor of the flume (Figure 3(a)). After about 5 waves, groups of spheres were organized and the pattern showed roughly perpendicular with the wave propagation direction (Figure 3(b)). A clear “particle wave” can be recognized after about 10 waves (Figure 3(c)). Then even exposed to ten more waves, the “particle wave” seemed to reach a stable state, which that the wave length of the particle wave become constant (Figure 3(d)).

Since the wave lengths of the particle waves are different with locations, a mean value on an image was obtained by considering three lines along the wave propagation direction, shown as Figure 4. For all the experiments, the relation between the dimensionless stable particle wave length, p_m/D , and the dimensionless wave bottom water particle excursion distance, $2a/D$, was plotted as Figure 5. The so called “stable particle wave length”, p_m , is the wave length calculated via the image when particle waves reach an equilibrium state, as shown in Figure 3(d). It indicated that the present experimental results agreed well with the relation proposed by Kaneko and Honji (1979a), shown below:

$$p_m/D = 3.5(2a/D)^{1/2} \quad (11)$$

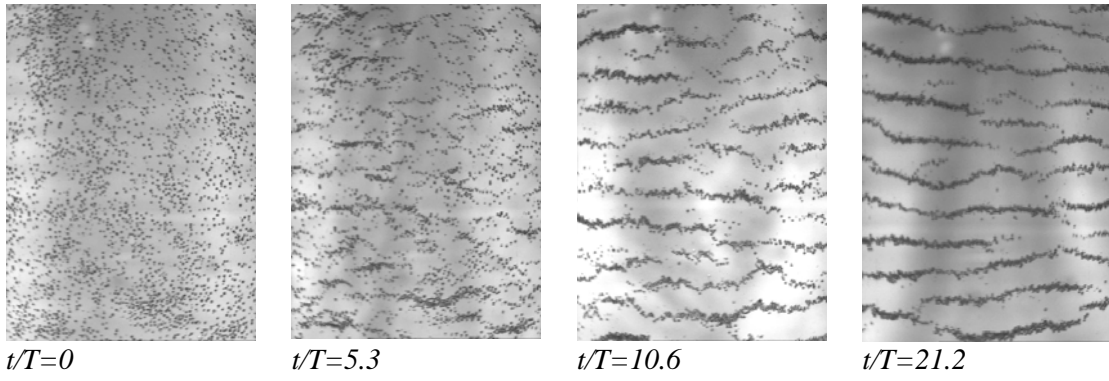
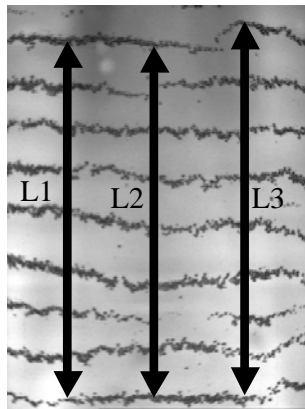


Figure 3 The evolution processes of initially scattering plastic resin spheres subjected to waves (case T5).



$$\lambda = \left(\frac{L_1}{n_1} + \frac{L_2}{n_2} + \frac{L_3}{n_3} \right) \div 3$$

Figure 4 Calculating the wave length of particle waves. n_1 , n_2 and n_3 are wave numbers along each line.

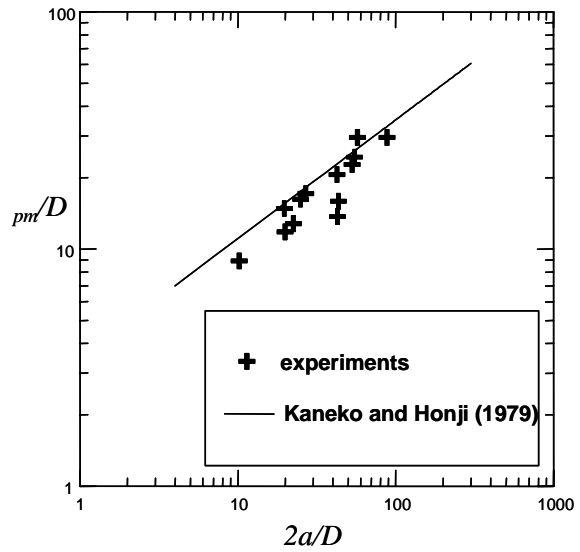


Figure 5 The relation between the dimensionless stable particle wave length and the dimensionless wave bottom water particle excursion distance.

The wavelengths of particle waves were further compared with those of sandy ripples. Sato et al. (1988) proposed that the dimensionless stable sandy ripple length can be expressed by a function composed of the relative roughness, $D_{50}/2a$, and Shields parameter, shown as eq. (12)

$$\frac{\lambda_{sm}}{2a} = 1.4 \left(2a/D_{50} \cdot \psi^{0.5} \right)^{-0.146} \quad (12)$$

where λ_{sm} is a stable sandy ripple length.

Figure 6 shows that under the same relative roughness and Shields parameter, the wavelength of a particle wave is obviously smaller than that of a sandy ripple. A fitting curve based on the experimental data was derived, as shown in eq. (13). According to Hwung and Hwang, (1997), as waves propagate on a thick layer of an initially leveled sand bed ($\sim 200 D_{50}$ of quartz sand, $D_{50}=0.2$ mm), the sand bed would evolve to organized sandy strips then rolling-grain ripples, then three dimensional vortex ripples and finally reach equilibrium two dimensional vortex ripples. The evolving ripple length grows exponentially with time elapsed. Since the particle waves in present study formed only by a single layer of spheres, moreover, spherical particles are not possible to pile up on a plane floor, it is of reason that the stable particle wave length smaller than that of a stable sandy ripple.

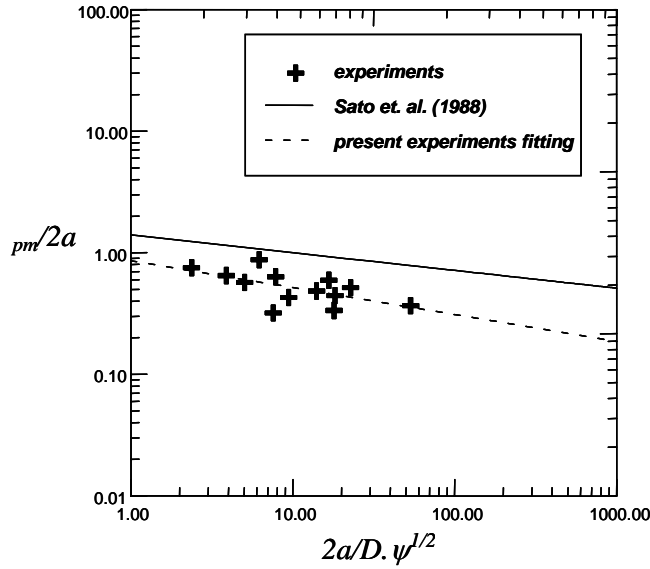


Figure 6 The relation between the dimensionless stable particle wave length and Shields parameter.

$$\frac{\lambda_{pm}}{2a} = 0.86(2a/D \cdot \psi^{0.5})^{-0.221} \quad (13)$$

Three examples of the sphere locations at the end of each wave cycle for cases with a single sphere are displayed in Figure 7. The horizontal axis is the displacement in traverse direction, which normalized by the width of the flume, B ; while the vertical axis is the displacement in longitudinal direction, which normalized by the water particle excursion distance at bottom, a . First of all, it apparently shows that the particle moved in both longitudinal and traverse directions. However, the traverse displacement of a sphere exhibited randomly through out the whole testing program. In case T4, which a plastic resin sphere was used, the traverse component of displacements are small and the directions were not consistent. Under almost the same waves as case T4, when the density of the sphere became larger (glass bead, case T9), the traverse component of displacements became much more remarkable and the sphere kept moving toward one lateral direction. With the same glass bead but increase the driving force (case T10), in spite of the more displaced distance in longitudinal direction, the traverse component of displacements did not change much in magnitude but the sphere kept moving toward the opposite lateral direction with respect to that of case T9. Conducting experiments with a single sphere needed to pay highly attention. The initial conditions as well as the boundary conditions all have to be checked and maintained in a fine quality with precise control. We still did not find a proper relation to describe the traverse displacement of a single sphere motion under waves in terms of the parameters discussed above. However, the relative intensity between the stress by the flow and the inertia force of the sphere must play a very important role. When Shields parameter is larger, that is, when the stress by the flow dominates the sphere motion, asymmetric wakes and hence the imbalance in traverse direction may force the sphere to move in either of the traverse directions, which depends strongly on any micro-changes of the flow-sphere interactions. On the other hand, when Shields parameter is smaller that the inertia of the sphere becomes relatively important, once the flow trigger the sphere to move, it may follow the moving trend at the onset of motion. In addition to the flow-sphere interaction problems, the moving mode of the sphere is another issue needed to be discussed. In our eyewitness and also through the imaging system records, the moving mode for the single sphere is simply rotational. Were there coupled with slightly sliding motion which may not noticeable by naked eyes or the 30 frames/s sampling rate of a camera? To look more detail into the spherical particle motion, a high-speed camera with frame rate up to 1,000 frames/s or faster would be a great help. Then the transport mode of the spheres can be well revealed.

Referring to the definition sketch illustrated in Figure 8, a sphere transported from position I to position II then to position III completes a wave cycle. We defined the net longitudinal displacement of a sphere in a wave cycle to be X , the one in traverse direction to be Y and the longitudinal displacement amplitude in a wave cycle to be A . The averaged net longitudinal displacement, \bar{X} , was obtained by taking the mean value of the net longitudinal displacements and the longitudinal displacement amplitudes in each wave cycles respectively. The averaged net longitudinal displacement against Shields parameter is displayed in Figure 9. And the relations can be expressed as eq. (14).

$$\frac{\bar{X}}{a} = 0.058 \left(\frac{a}{D} \cdot \psi^{\frac{1}{2}} \right)^{0.812} \quad (14)$$

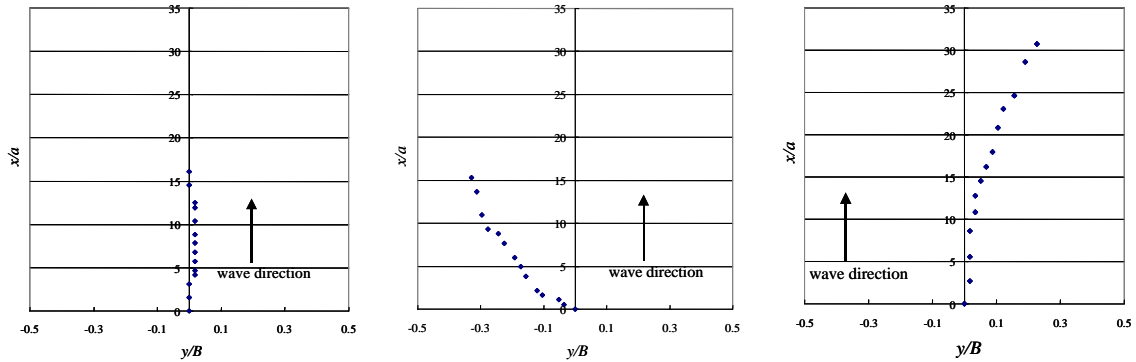


Figure 7 The locations at the end of each wave cycle of a single sphere (left: case T4; center: T9; right: T10)

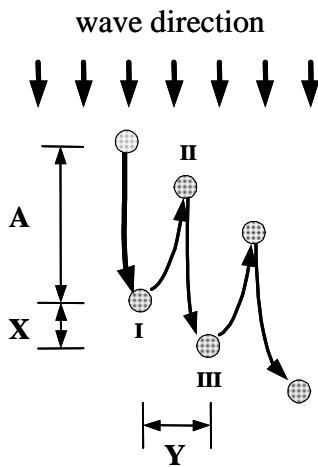


Figure 8 Definition figure of X , Y and A .

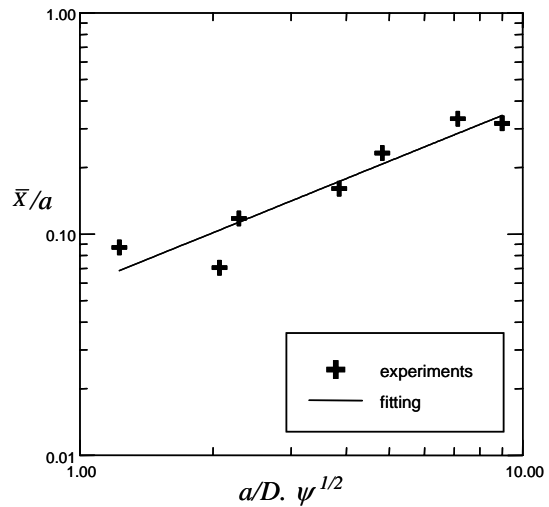


Figure 9 The relation between the averaged net longitudinal displacement and Shields parameter.

5. CONCLUSIONS

The motion of spheres initially rested on a plane floor then subjected to waves was investigated. The spherical particles would form a periodic pattern in space called particle waves as they experienced a couple waves. The relation between the dimensionless stable particle wavelength and the dimensionless water particle excursion distance at bottom agreed well with eq.(11), which was proposed by Kaneko and Honji (1979a). The path records of a

single sphere show that the spherical particle would move in both longitudinal and traverse directions. Its mean forward components in longitudinal direction are proportional with Shields parameter. But the traverse component of displacement exhibited randomly. Both the flow-sphere interaction problems and the modes of spheres moving on a plane floor under waves are needed with further investigation.

ACKNOWLEDGEMENT

This work was financially supported by the Research Center of Ocean and Environment of National Cheng Kung University, under the Project of Promoting Academic Excellence & Developing World Class Research Centers. The authors would also like to express sincerely gratitude to the staffs in Tainan Hydraulics Laboratory for their technical supports.

REFERENCES

- Bagnold, R. A. (1946), Motions of waves in shallow water; interaction between waves and sand bottoms, *Proceeding of Royal. Soc., London, Ser. A*, vol. 187, pp.1-15.
- Chang E. J. , M.R. Maxey (1994), Unsteady-flow about a sphere at low to moderate Reynolds-number .1. Oscillatory motion, *Journal of Fluid Mechanics*, vol. 277, pp. 347-379
- Hwang, Kao-Shu (1995), The formation and the flow fields of wave-induced sandy ripples, Phd. thesis.
- Hwung, H.H. and K.S. Hwang (1997), Transient process of wave induced sandy ripples, *Journal of the Chinese Institute of Civil and Hydraulics Engineering*, vol. 9, No. 1, pp. 119-127.
- Kaneko, A. and H. Honji (1979a), Initiation of ripple marks under oscillating water, *Sedimentology*, vol. 26, pp.101-113.
- Kaneko, A. and H. Honji (1979b), Double structures of steady streaming in the oscillatory viscous flow over a wavy wall, *Journal of Fluid Mechanics*, vol. 93, pp. 347-367.
- Johnson T. A. and V. C. Patel (1999), Flow past a sphere up to a Reynolds number of 300, *Journal of Fluid Mechanics*, vol. 378, pp. 19-70.
- Joseph D. D., Y. J. Liu, M. Poletto and J. Feng (1994), Aggregation and Dispersion of Spheres Falling in Viscoelastic Liquids, *J. Non-Newtonian Fluid Mech.*, vol. 54, pp. 45-86.
- Martin C. S., M. Padmanabhan and C. D. Ponce-Campos (1976), Rolling motion of a sphere on a plane boundary in oscillatory flow, *Journal of Fluid Mechanics*, vol. 76, pp. 653 - 674.
- Sarpkaya, T., (1975), Forces on Cylinders and Spheres in a Sinusoidally Oscillating Fluid, *Journal of Applied Mechanics*, ASME, vol. 42, pp. 32-37
- Sato, S., Mitani, K. and A. Watanabe (1988), Geometry of sandy ripples and net sand transport rate due to regular and irregular oscillatory flows, *Coastal Engineering in Japan*, vol.30, No.2. pp. 89-98.
- Sleath, J. F. A. (1976), On rolling grains ripples, *Journal of Hydraulic Research*, vol. 14, pp. 69-81.
- Sun R. and A. T. Chwang (2006), Inactions and collisions of two solid spheres in the gravitational environment, *Proceeding of the 7th International Conference on Hydrodynamics*, pp. 3-10.
- Vasseur, P. and R.G. Cox (1977), The lateral migration of spherical particles sedimenting in a stagnant bounded fluid, *Journal of Fluid Mechanics*, vol. 80, pp. 561-591.
- Wunenburger R., V. Carrier, and Y. Garrabos (2002), Periodic order induced by horizontal vibrations in a two-dimensional assembly of heavy beads in water, *Physics of Fluids*, vol. 14, pp. 2350"